

# New Retrieval Algorithm for Deriving Land Surface Temperature from Geostationary Orbiting Satellite Observations

Li Fang, Yunyue Yu, Hui Xu, and Donglian Sun

**Abstract**—Accurate derivations of land surface temperature (LST) and land surface emissivity (LSE) from satellite measurements are difficult because the two variables are closely coupled. Features of significant/insignificant temporal variations in LST/LSE are recognized to de-couple both values using multiple-temporal satellite observations over the same geolocation. In this paper, a new approach is presented for deriving LST and LSE simultaneously by using multiple-temporal satellite observations. Two split-window regression formulas are carefully selected for the approach, and two satellite observations over the same geolocation within a certain time interval are utilized. The method is particularly applicable to geostationary satellite missions from which qualified multiple-temporal observations are available. The approach is designed and implemented for generating the LST and LSE values from the U.S. geostationary operational environmental satellite (GOES) eight imager data and the European meteorological second generation (MSG) mission spinning enhanced visible and infrared imager (SEVIRI) data. The performance of the algorithm is evaluated in terms of both accuracy and sensitivity. The retrieval results are compared against ground-truth observations from the U.S. Atmospheric radiation measurement facility and six surface radiation budget network (SURFRAD) stations. The validation results show the LST retrieval accuracy is around 1.95 K with good correlations of up to 0.9038. The method is applicable to the future U.S. GOES-R mission as well as the MSG mission considering that the advanced baseline imager (ABI) onboard the GOES-R satellites and the SEVIRI onboard the MSG satellite have similar split-window bands.

**Index Terms**—Geostationary operational environmental satellite (GOES), land surface emissivity (LSE), land surface temperature (LST), matrix inversion approach.

Manuscript received September 11, 2010, revised December 22, 2012; accepted January 15, 2013. Date of publication March 21, 2013; date of current version December 12, 2013. This work was supported by the National Oceanic and Atmospheric Administration (NOAA) GOES-R Satellite Algorithm/Application Working Group. The manuscript contents are solely the opinions of the authors and do not constitute a statement of policy, decision, or position on behalf of the NOAA or the U.S. Government agencies.

L. Fang and D. Sun are with the Department of Geography and Geoinformation Science, College of Science, George Mason University, Fairfax, VA 22030 USA (e-mail: lfang1@gmu.edu; dsun@gmu.edu).

Y. Yu is with the National Environmental Satellite, Data, and Information Service Center for Satellite Applications and Research, National Oceanic and Atmospheric Administration, College Park, MD 20740 USA (e-mail: yunyue.yu@noaa.gov).

H. Xu is with I. M. Systems Group, Inc., College Park, MD 20740 USA (e-mail: hui.xu@noaa.gov).

Color versions of one or more of the figures in this paper are available online at <http://ieeexplore.ieee.org>.

Digital Object Identifier 10.1109/TGRS.2013.2244213

## I. INTRODUCTION

LAND surface temperature (LST), as a key parameter for the Earth's surface energy balance is of great value to research in the fields of climatology, hydrology, meteorology, ecology; for example, Running *et al.* [1] studied the process of surface-atmosphere interactions using LST as one of the important parameters. Satellite LST retrieval provides the feasibility of producing continuous global surface temperature data sets.

High resolution satellite LST retrieval is usually performed at thermal infrared (TIR) wavelengths using multi-channel technique, where temperature and emissivity separation (TES) is a fundamental problem. In general, surface emitted TIR radiance is dependent on both surface temperature and emissivity, where the latter also varies with wavelength. This is particularly true for most land surfaces where emissivity can be significantly less than unity. The problem of LST retrieval from TIR measurements cannot be solved simply by adding observations at different wavelengths, because the number of unknowns is always at least one more than the measurements [2]–[4]. Several attempts have been made to solve this underdetermined problem by additional constraints or prior knowledge, such as spectral ratio method [5] and Alpha coefficients method [6]. In particular, Wan and Li [7] presented a numerical method for separating LST and emissivity utilizing MODerate-resolution imaging spectroradiometer (MODIS) onboard the NASA's earth observing system (EOS) satellites, which initiated the TES practice using multiple observations and/or multiple spectral channels [8] and [9]. Liang [4] further developed an optimization procedure to constrain errors in the simultaneous determination process for LST and emissivity. Other techniques, such as the neural network method [10] has been tried to solve the ill-posed problem by extracting potential information from training datasets.

All the above methods for simultaneous retrieval of LST and land surface emissivity (LSE) depend on a well-determined or over-determined matrix problem that is built on a multiple-channel dataset from the satellite infrared radiometer or imager and spectral radiative transfer equations [11]. Atmospheric profiles required for solving the radiative transfer equations are usually obtained through microwave sounder, and are usually in coarser spatial resolution than the infrared data. Solution of

the matrix problem may be unreliable as the method is known to be sensitive to noise of the input data [11] and [12]. In addition, intensive numerical computation time is required for processing the radiative transfer equations and for solving the matrix problem.

Recently, a similar TES procedure was applied to proxy images of the U.S. geostationary operational environmental satellite (GOES) R Series (GOES-R) satellites for producing land surface emissivity from its advanced baseline imager (ABI) [13]. A split-window (SW) algorithm is applied to the GOES-R LST retrieval, in which the surface emissivities at the two TIR channels are assumed [14]. It is assumed that the high quality LST database will be available by the time the GOES-R is in operation.

In this paper, we present a simplified TES method, the matrix inversion approach (MIA), based on two satellite observations. Instead of applying the radiative transfer model and the atmospheric profiles for building up the matrix inversion problem, two SW LST algorithms, which were evaluated in the GOES-R LST algorithm development, are utilized to derive LSTs at two time stamps and emissivities at two TIR channels. The method was briefly reported in 2009 [9]; this paper shows theoretical details and some evaluation results.

The outline of this paper is as follows. Section II introduces the principle and implementation of the method. Section III gives initial results of the method applied to GOES-8 and the spinning enhanced visible and infrared imager (SEVIRI) data. A validation effort is made by comparing the retrieved LST with the ground truth temperature measurements in Section IV. Sensitivity analysis is provided in Section V. Finally, discussions and conclusions are presented in Sections VI and VII, respectively.

## II. METHOD

Wan and Li [7] first developed a two-measurement algorithm for deriving LST and LSE simultaneously using polar orbiting satellite measurements of infrared channels. The basic assumption of this method is that during the two-time measurements (i.e., day and night for the polar orbiting satellite), the surface emissivities of infrared channels remain the same. Limitations of this method have been discussed in the LST community. First, the two-measurement method requires the measurements from the day and night observations. Since the polar orbiting satellite is capable of providing only one observation for each case, the retrieval availability is greatly limited especially when taking cloud condition into account. Second, the algorithm is much affected by the assumption that emissivity of each infrared channel does not vary from daytime to nighttime. In addition, the algorithm relies on atmospheric profile, which is obtained in a coarse resolution and may introduce significant errors, for solving the radiative transfer equations.

However, it is a promising attempt to extend this two-measurement approach to extract LST from geostationary-orbiting satellite observations. High temporal refresh rate of the GOES satellite observation not only ensures a significantly large number of the cloud-free data pairs for the retrieval

availability, but also supports the assumption that the surface emissivity remains the same between a short temporal interval. If dependency on the radiative transfer process can be excluded from the two-measurement method, which also implies that the real-time atmospheric profile information is not needed, it would be ideal applying this approach to the GOES satellite mission. To reach this goal, a basic principle of the MIA is briefly introduced here.

Assuming that there are two established algorithms,  $F()$  and  $G()$ , for deriving the satellite LST ( $T_s$ ) for a given pixel. In our case,  $F()$  and  $G()$  represent two linear SW LST algorithms. When applying these two algorithms to two measurements at two different times at  $t_1$  and  $t_2$ , we have

$$\begin{aligned} T_{s,t_1} &= f_0(T_{11,t_1}, T_{12,t_1}, \theta_{t_1}) \\ &\quad + f_1(T_{11,t_1}, T_{12,t_1}, \theta_{t_1})X_1(\varepsilon_{11}, \varepsilon_{12}) \\ &\quad + f_2(T_{11,t_1}, T_{12,t_1}, \theta_{t_1})X_2(\varepsilon_{11}, \varepsilon_{12}) \\ T_{s,t_2} &= g_0(T_{11,t_2}, T_{12,t_2}, \theta_{t_2}) \\ &\quad + g_1(T_{11,t_2}, T_{12,t_2}, \theta_{t_2})X_1(\varepsilon_{11}, \varepsilon_{12}) \\ &\quad + g_2(T_{11,t_2}, T_{12,t_2}, \theta_{t_2})X_2(\varepsilon_{11}, \varepsilon_{12}) \end{aligned} \quad (1)$$

where  $T_{11,t_i}$  and  $T_{12,t_i}$  are the brightness temperatures measured by the satellite sensors around 11 and 12  $\mu\text{m}$  at time  $t_i$ ;  $\varepsilon_{11}, \varepsilon_{12}$  are the emissivities at the two channels;  $\theta_{t_i}$  is the satellite view zenith angle at time  $t_i$ , and  $\theta_{t_1}$  and  $\theta_{t_2}$  are the same for the geostationary satellite sensor observing a certain ground area; functions  $f_j()$  and  $g_j()$  ( $j = 0, 1, 2$ ) are certain brightness temperature dependencies in the two SW LST algorithms  $F()$  and  $G()$ , respectively;  $X_1(\varepsilon_{11}, \varepsilon_{12})$  and  $X_2(\varepsilon_{11}, \varepsilon_{12})$  are fixed relationships derived from  $\varepsilon_{11}$  and  $\varepsilon_{12}$ , such as  $X_1(\varepsilon_{11}, \varepsilon_{12}) = \varepsilon_{11} + \varepsilon_{12}/2$ .

These independent equations can be posed as a linear algebra problem in the matrix form:

$$a\mathbf{X} = b \quad (2)$$

where  $\mathbf{X} = (T_{s,t_1}, T_{s,t_2}, X_1, X_2)$ . To be more specific,

$$\begin{aligned} &\begin{bmatrix} 1 & 0 & -f_1(T_{11,t_1}, T_{12,t_1}, \theta) & -f_2(T_{11,t_1}, T_{12,t_1}, \theta) \\ 1 & 0 & -g_1(T_{11,t_1}, T_{12,t_1}, \theta) & -g_2(T_{11,t_1}, T_{12,t_1}, \theta) \\ 0 & 1 & -f_1(T_{11,t_2}, T_{12,t_2}, \theta) & -f_2(T_{11,t_2}, T_{12,t_2}, \theta) \\ 0 & 1 & -g_1(T_{11,t_2}, T_{12,t_2}, \theta) & -g_2(T_{11,t_2}, T_{12,t_2}, \theta) \end{bmatrix} \begin{bmatrix} T_{s,t_1} \\ T_{s,t_2} \\ X_1 \\ X_2 \end{bmatrix} \\ &= \begin{bmatrix} f_0(T_{11,t_1}, T_{12,t_1}, \theta) \\ g_0(T_{11,t_1}, T_{12,t_1}, \theta) \\ f_0(T_{11,t_2}, T_{12,t_2}, \theta) \\ g_0(T_{11,t_2}, T_{12,t_2}, \theta) \end{bmatrix}. \end{aligned} \quad (3)$$

There are four unknowns ( $T_{s,t_1}, T_{s,t_2}, \varepsilon_{11}$  and  $\varepsilon_{12}$ ) in the matrix  $\mathbf{X}$ , which can be solved uniquely if the equations are not singularly posed. Thus, the algorithms  $F()$  and  $G()$  must be independent, and the two measurement ( $T_{11,t_1}, T_{12,t_1}$ ), ( $T_{11,t_2}, T_{12,t_2}$ ) must be significantly different. To avoid singularity in the MIA, temperatures at the two selected times should have significant difference, while the emissivities at the two-measurement times should remain the same.

In our application, two SW LST algorithms are utilized as these established linear regression formulas,  $f()$  and  $g()$ .

Assuming  $f()$  represents the SW LST algorithm developed by Wan and Dozier in 1996 [15], which is mathematically written as

$$\begin{aligned} T_s = & C + \left( A_1 + A_2 \frac{1 - \varepsilon}{\varepsilon} + A_3 \frac{\Delta \varepsilon}{\varepsilon^2} \right) (T_{11} + T_{12}) \\ & + \left( A_4 + A_5 \frac{1 - \varepsilon}{\varepsilon} + A_6 \frac{\Delta \varepsilon}{\varepsilon^2} \right) (T_{11} - T_{12}) \\ & + D(T_{11} - T_{12})(\sec \theta - 1). \end{aligned} \quad (4)$$

Again, in (4),  $T_{11}$  and  $T_{12}$  represent the top-of-atmosphere brightness temperatures of the TIR channels at 11 and 12  $\mu\text{m}$ , respectively;  $\varepsilon_{11}$  and  $\varepsilon_{12}$  are the spectral emissivity values of the land surface at ABI channels 14 and 15, respectively;  $\varepsilon = (\varepsilon_{11} + \varepsilon_{12})/2$  and  $\Delta \varepsilon = \varepsilon_{11} - \varepsilon_{12}$ ;  $C$ ,  $A_1 - A_6$ , and  $D$  are coefficients; a path-length correction term  $(T_{11} - T_{12})(\sec \theta - 1)$  is used to minimize the water vapor effects with increasing view angle of the satellite, which cannot be ignored to geostationary orbit satellites with high orbit altitude [16]. Equation (4) can be rearranged in the MIA in terms of the unknown matrix  $X$ , which is

$$\begin{aligned} T_s = & [C + A_1(T_{11} + T_{12}) - A_2(T_{11} + T_{12}) \\ & + A_4(T_{11} - T_{12}) - A_5(T_{11} - T_{12}) \\ & + D(T_{11} - T_{12})(\sec \theta - 1)] \\ & + [A_2(T_{11} + T_{12}) + A_5(T_{11} - T_{12})]X_1 \end{aligned} \quad (5)$$

where  $X_1 = 1/\varepsilon$  and  $X_2 = \Delta \varepsilon/\varepsilon^2$ .

Similarly, if  $g()$  stands for the SW LST algorithm developed by Vidal in 1991 [17], which is written as

$$\begin{aligned} T_s = & C + A_1 T_{11} + A_2 (T_{11} - T_{12}) + A_3 \frac{1 - \varepsilon}{\varepsilon} + A_4 \frac{\Delta \varepsilon}{\varepsilon^2} \\ & + D(T_{11} - T_{12})(\sec \theta - 1). \end{aligned} \quad (6)$$

Then, the formula will be adapted in the MIA as

$$\begin{aligned} T_s = & C + A_1 T_{11} + A_2 (T_{11} - T_{12}) - A_3 \\ & + D(T_{11} - T_{12})(\sec \theta - 1) + A_3 X_1 + A_4 X_2. \end{aligned} \quad (7)$$

Again,  $X_1$  and  $X_2$  denote  $1/\varepsilon$  and  $\Delta \varepsilon/\varepsilon^2$ , respectively. In our application, all the SW LST algorithms selected for the MIA are stratified atmospheric conditions (dry/moist) and illumination conditions (daytime/nighttime).

Similar to the combination of Wan and Dozier and Vidal's algorithms (Combination A), another combination of two algorithms (Coll and Caselles, 1997 [18] and Price, 1984; Combination B) is derived and implemented for comparison. The formula and coefficients of these SW algorithms are listed in Appendix. Among currently available SW LST algorithms [15], [17], [19]–[26], some other combinations are also feasible to the MIA (e.g., the combination of Ulivieri's [25] and Sobrino's [24]). However, some are not appropriate for this method because of potential singularity problems or computational complexity.

### III. EXPERIMENT AND RESULTS

#### A. Experiment on SEVIRI Data

SEVIRI has two TIR channels with central wavelengths of 10.8 and 12.0  $\mu\text{m}$ , which can be applied to the SW LST

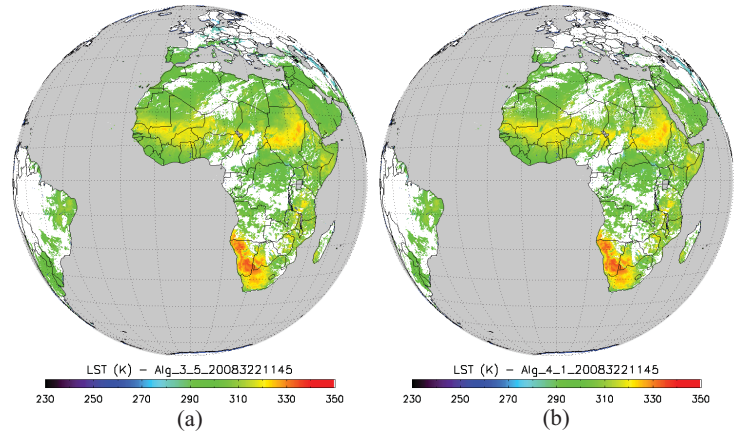


Fig. 1. New algorithm is applied to SEVIRI data for LST retrievals at 11:45 GMT on Nov. 17, 2008, using (a) Combination A and (b) Combination B.

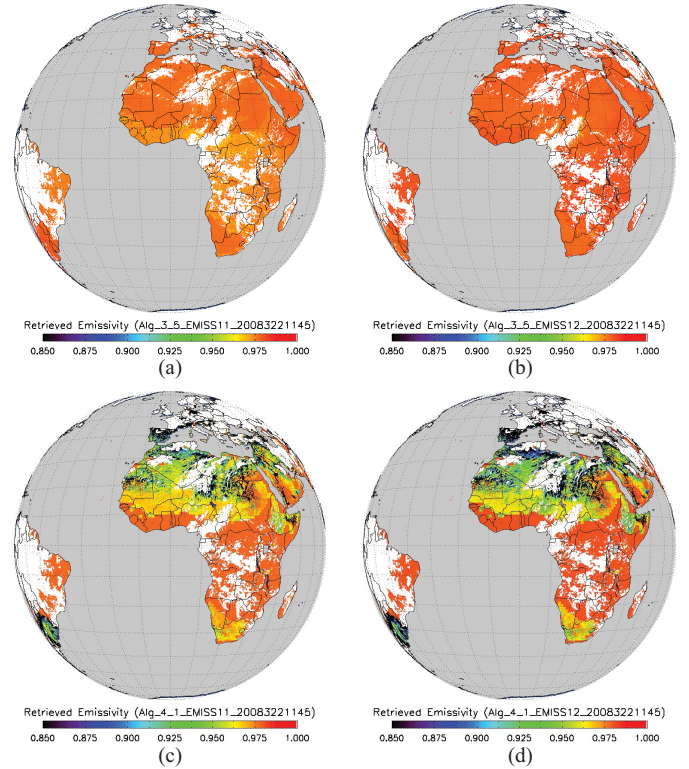


Fig. 2. Retrieved emissivity maps for the SEVIRI channels at 10.8 and 12.0  $\mu\text{m}$  from different algorithm combinations. (a) Emissivity at 10.8  $\mu\text{m}$  using SW Combination B. (b) Emissivity at 12  $\mu\text{m}$  using SW Combination B. (c) Emissivity at 10.8  $\mu\text{m}$  using SW Combination A. (d) Emissivity at 12  $\mu\text{m}$  using SW Combination A.

algorithms. The MIA is applied to two time stamps (11:45 and 12:45 GMT on Nov. 17, 2008) of SEVIRI data at these two TIR channels. Only cloud-free pixels participate in the inverse process, since SW LST algorithms do not work well in cloudy conditions.

The derived LST maps at 11:45 GMT using Combination A and Combination B are shown in Fig. 1. The areas in white are cloudy pixels. For the winter season, the temperature over the Southern Hemisphere is relatively higher than that over the Northern Hemisphere, with localized hot-spots in the Namib

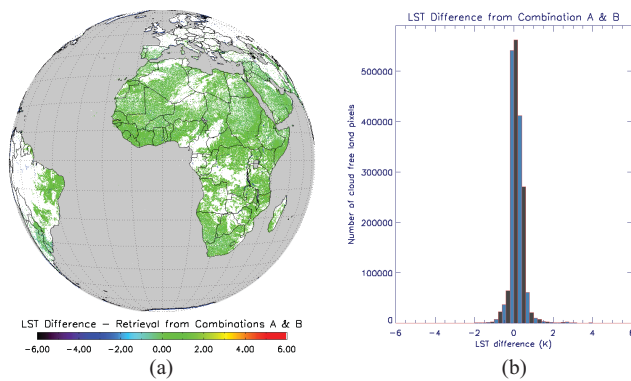


Fig. 3. (a) Map of differences and (b) histogram of differences in the LST retrievals at 11:45 GMT on Nov. 17, 2008 from Combinations A and B.

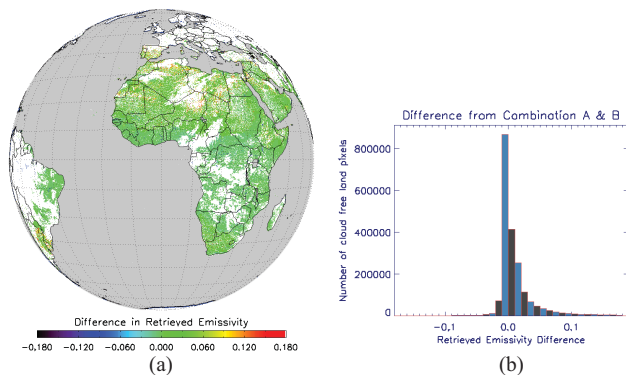


Fig. 4. (a) Map of differences and (b) histogram of differences in the emissivity retrievals at 10.8 and 12  $\mu\text{m}$  from Combinations A and B.

Desert and Kalahari Desert areas. The Sahel, a desertification area between the Sahara desert and the Sudanian savannas is slightly warmer than the tropical rainforests region in central Africa. The simultaneously retrieved emissivities at 10.8 and 12.0  $\mu\text{m}$  based on these two combinations are shown in Fig. 2. More stable emissivity retrievals are obtained by the algorithms of Combination A, which not only captures reasonable emissivity distribution but also shows possible changing details. The regions covered by dense vegetation possess high emissivity values, such as tropical rainforests in central Africa and eastern littoral in Brazil, while desert regions apparently own low values, such as the vast area in the Sahara Desert, arid region of Sahel, and rugged mountain region in southeastern Brazil.

For showing differences in the retrieved LST results using different algorithm combinations, comparison between the two algorithm combinations is represented in graphic view in Fig. 3 on the left, and the statistical distribution of the difference is shown on the right. Similarly, differences in the retrieved emissivities are shown in Fig. 4, graphically on the left and statistically on the right. The variation in LST retrieval is very minor, with over 95% pixels within 0.5 K. This implies the stability of this method. For the experiment on GOES data and the following validation effort, Combination A is applied and tested only.

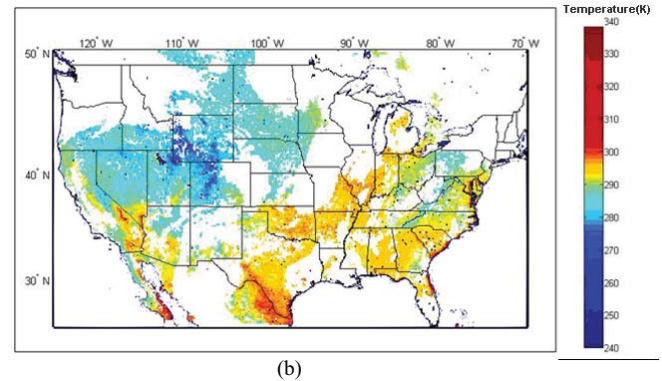
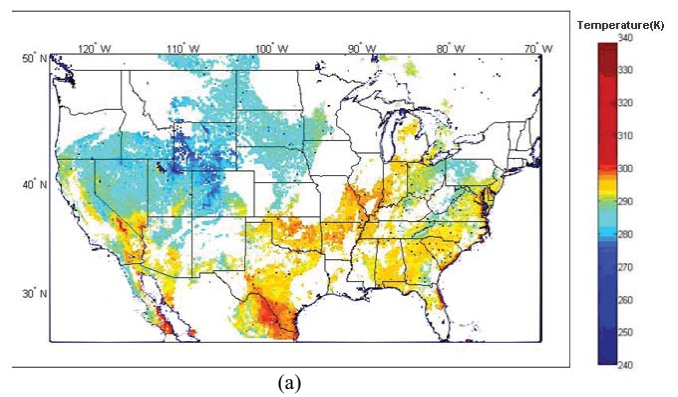


Fig. 5. New algorithm is applied on GOES-8 Imager data for LST retrievals at (a) 9 a.m. and (b) 10 a.m. on July 14th, 1997.

### B. Experiment on GOES Data

ABI onboard the GOES-R satellites will acquire data in 16 channels from the visible to infrared wavelengths, of which two TIR channels centered at 11.2 (Channel 14) and 12.3  $\mu\text{m}$  (Channel 15) are designed especially for LST retrieval. Considering that the current GOES-8 Imager data is utilized as proxy data for GOES-R LST algorithm development, it is used for evaluating this method as well. It is desired that the method is applicable for the GOES-R mission.

The new TES method using Combination A is applied to the two GOES-8 observations acquired at 9:00 a.m. and 10:00 a.m. on July 14th, 1997. Similar to the application on SEVIRI, cloud-free pixels are chosen for inversion based on cloud mask (available from NOAA GOES Surface and Insolation Products). Fig. 5 shows the LST retrievals at 9 a.m. and 10 a.m., and Fig. 6 shows the retrieved emissivities at 11 and 12  $\mu\text{m}$ .

The spatial variation of retrieved temperatures shown in Fig. 5 is mostly latitudinal. The majority of the southern area is warmer than the northern counterpart. The highest temperatures appeared in the region of low latitudes, like southern Texas, besides extremely high temperatures detected in the arid, hot desert in southeastern California. The emissivity of northwestern U.S. Continent is generally higher than that of southeastern U.S. This distribution is similar to that of the MODIS monthly emissivity product [27].

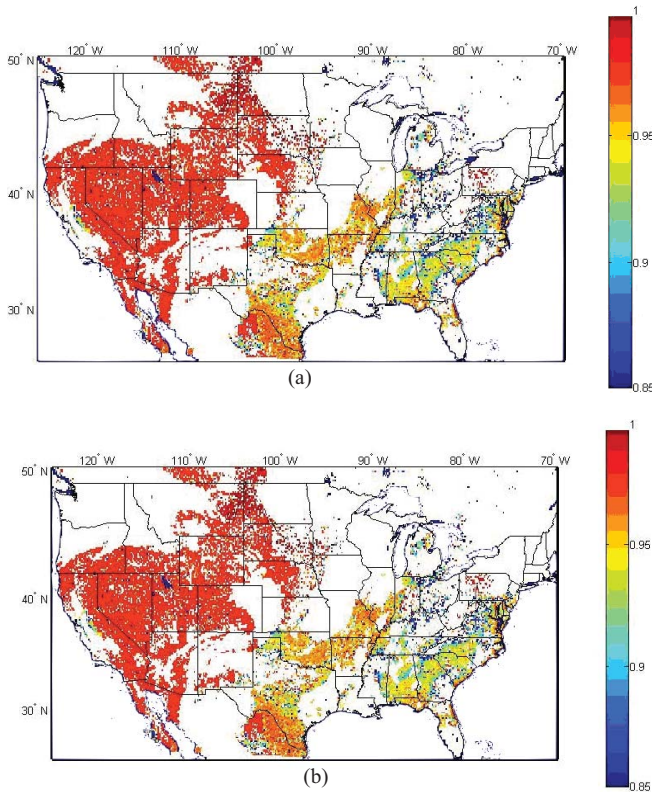


Fig. 6. Retrieved emissivity at (a) 11 and (b) 12  $\mu\text{m}$  on July 14th, 1997.

IV. VALIDATIONS

Validation of satellite LST retrievals is always challenging due to a verity of reasons. The spot-to-pixel variance is one of them. The mismatch of ground point measurement and 4-km GOES pixel in validation process itself is a big topic. The ground LST measurements particularly for LST validation purpose (e.g., field campaign) are rare and very expensive. It is almost impossible trying to use them for a comprehensive LST validation study (i.e., with enough number of data pairs for statistical significance and covering difference atmospheric/seasonal/geographic conditions). While researchers are conducting studies on such problems [16], the spot measurements of ground data are still being widely used for general evaluation of the satellite LST products. In this paper, we followed the traditional validation approach of using ground measurements, including the U.S. Atmospheric Radiation Measurement (ARM) and Surface Radiation Budget Network (SURFRAD). The observations from ARM and SURFRAD have also been used by many other scientists to validate satellite-based LST retrievals [28]–[30], partly because of their operational availability, providing large amount of data covering enough long time.

Although the proposed method derives the LST and LSE simultaneously, it is worth noticing that the focus in this paper is LST retrievals. The advantage of MIA is trying to develop a method of LST derivation without knowing the LSE prior. The comprehensive validation of LSE is more complicated than that of LST. We were not trying to validate both LST

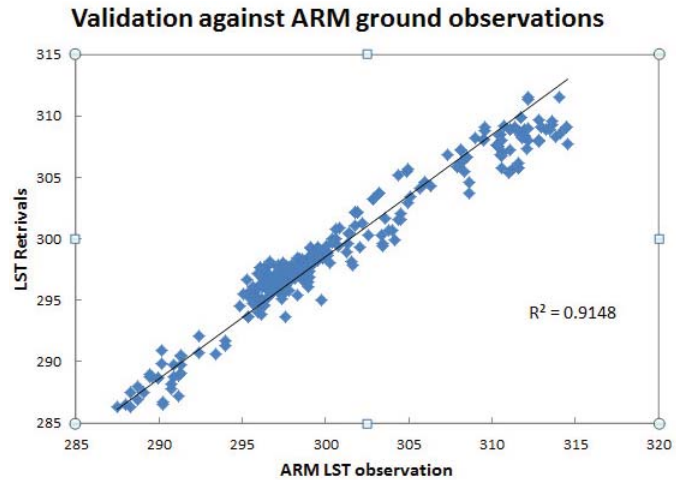


Fig. 7. Validation results for the LST retrievals, using the dataset from U.S. atmospheric radiation measurement (ARM) facility.

TABLE I  
LIST OF ARM AND SURFRAD OBSERVATION SITES

Site No.	Site Location	Lat(N)/Lon(W)	Surface Type*
1	ARM	36.607/97.489	Partial vegetation
2	Bondville, IL	40.05/88.37	Crop land
3	Fort peck, MT	48.31/105.10	Grass land
4	Goodwin creek, MS	34.25/89.87	Deciduous forest
5	Table mountain, CO	40.13/105.24	Crop land
6	Desert rock, NV	36.63/116.02	Open Shrub land
7	Pennsylvania state university, PA	40.72/77.93	Mixed forest

and LSE in a single paper. Therefore, the validation effort focused on LST retrievals in this paper.

A. Validations Against ARM Ground Data

The Near-Surface Observation Data Set-1997 (NESOB-97) from ARM facility is utilized to validate the LST retrievals from the new TES retrieval algorithm. The continuous temperature observations with thirty-minute interval were acquired at the ARM Cloud and Radiation Testbed (ARM/CART) site, which is located at Lamont, Oklahoma (36.607°N, 97.489°W). A brief description about ARM site is presented in Table I. Multi-filter radiometer is used to detect the diffuse/total upwelling irradiance, which is then converted to the skin temperature based on the NOAA/Atmospheric Turbulence and Diffusion Division algorithm [31] and [32]. The error that may be introduced by the radiometer is about 5%.

The LSTs retrieved from cloud-free GOES-8 thermal infrared measurements over a whole month (July 1997) are compared with the ARM ground-based observations at the same location and at the same time. Fig. 7 shows the scatter plots of retrieval result for totally 317 cases. The mean absolute error and standard deviation of the difference of inversed and ARM measurements are 1.66 and 1.544 K,

TABLE II  
GROUND-BASED OBSERVATIONS AND RETRIEVED TEMPERATURES

Date	Retrieved Temperature	Ground-Observed	Absolute Differences	Retrieved Emissivity	Retrieved Emissivity
t1:9a.m.,	(RT)	Temperature (GT)	Between	at	at
t2:10a.m.	(K)	(K)	GT and RT	Channel 4	Channel 5
07/10/97 (t1)	295.82	295.48	0.34	0.96188	0.95387
07/10/97 (t2)	295.56	295.09	0.47	0.96188	0.95387
07/12/97 (t1)	296.14	296.24	0.10	0.97147	0.9684
07/12/97 (t2)	296.17	295.83	0.34	0.97147	0.9684
07/14/97 (t1)	296.62	297.18	0.56	0.93849	0.92109
07/14/97 (t2)	297.05	296.98	0.07	0.93849	0.92109
07/24/97 (t1)	297.33	297.66	0.33	0.96316	0.95656
07/24/97 (t2)	297.70	297.46	0.24	0.96316	0.95656
07/25/97 (t1)	297.86	297.16	0.70	0.95739	0.94943
07/25/97 (t2)	297.83	296.68	1.15	0.95739	0.94943
07/27/97 (t1)	296.68	297.44	0.76	0.96353	0.95398
07/27/97 (t2)	296.35	296.28	0.07	0.96353	0.95398
07/28/97(t1)	297.57	297.94	0.37	0.95829	0.94913
07/28/97(t2)	297.06	297.83	0.77	0.95829	0.94913

respectively. To take a closer look at the regression result, the retrieved LST and LSE, the ground-measured temperatures, as well as the biases of seven cases (as representatives) are listed in Table II. Overall, the satellite-retrieved temperatures match the ground observations very well. The skin temperature shows an overall increase by 1.24 K from July 1st to July 28th with smaller fluctuation in between. The retrieved emissivity at 11  $\mu\text{m}$  differs very little from that at 12  $\mu\text{m}$  with the mean absolute difference of merely 0.0088. We also notice from the retrieved emissivity that the emissivity varies within the month at the rate of 3.4%.

### B. Validations Against SURFRAD Data

Validation effort is further conducted by comparing retrievals against *in situ* measurements from SURFRAD. It continuously monitors components of the surface radiation budget, which is then converted to skin temperatures. References [33] and [34] give more information about the instruments and observations of SURFRAD. Brief information about SURFRAD experimental sites (e.g., site location, associated surface type) has been presented in Table I.

One month SURFRAD data (July, 2002) over six stations have been selected to validate the performance of MIA. Since LST retrieval algorithms are sensitive to cloud conditions, it is only applied to cloud-free pixels to calculate LSTs and emissivities. The cloud fractions datasets are available from NOAA GOES surface and insolation products (GSIP). Fig. 8 shows the scatter plot of the regression results of totally 2341 cloud-free cases. Validation effort against SURFRAD shows the similar accuracy to the ARM results. The mean absolute error and STD of differences between retrievals and ground observations is 2.32 and 1.953 K, respectively.

## V. SENSITIVITY ANALYSIS

The algorithm errors come from several sources. First, the algorithm may inherit the uncertainty of split-window

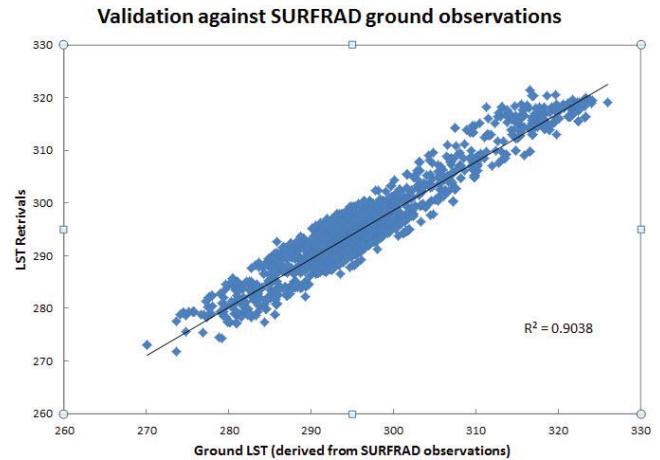


Fig. 8. Validation results for the LST retrievals, using the dataset from SURFRAD facility.

algorithms themselves. The accuracy and sensitivity of split-window have been carefully studied in previous literature. Nine split-window algorithms have been applied to GOES eight measurements, as a proxy for the new generation of GOES series, and the performance of these SW algorithms has been evaluated [14]. The result indicates that the uncertainty can be controlled at level of 0.5 K. Another error may be attributed to the singularity problem of the retrieval method, which would occur when the equations in the matrix problem are very close in value. In addition, the quality of algorithm input (BT observations) may also cause the uncertainty.

To quantitatively estimate the uncertainty brought in by the noise in BT observations, a simulation dataset has been built through a forward simulation process using MODerate resolution atmospheric TRANsmission (MODTRAN). To make the simulation dataset more representative, many variations have been taken into account, including characteristics of instrument, solar and satellite geometry, surface conditions, and atmospheric condition. After running the simulation process, 14 822 data pairs (two-time modeled brightness temperatures

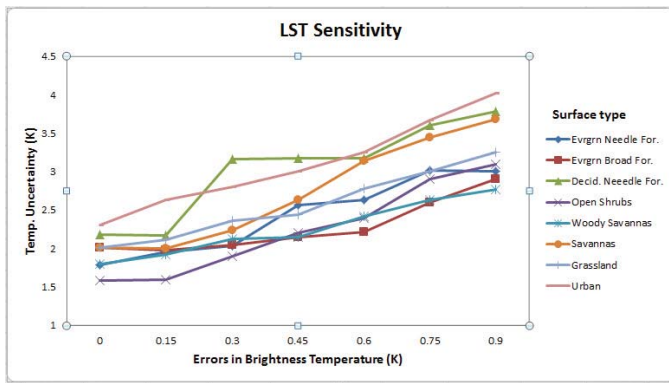


Fig. 9. LST sensitivity to sensor noise for different surface types.

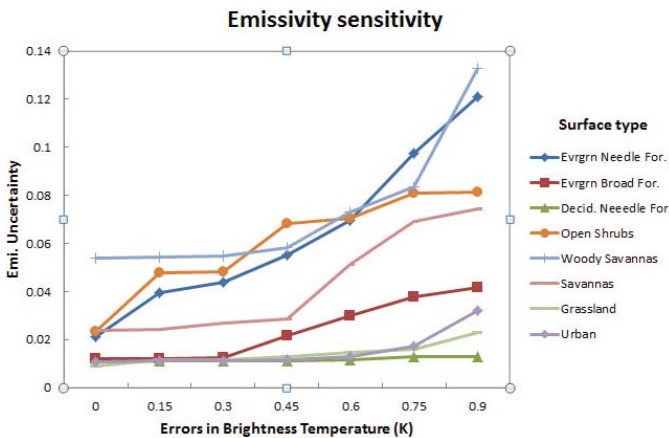


Fig. 10. Emissivity sensitivity to sensor noise for different surface types.

TABLE III  
INFORMATION ABOUT SIMULATION DATASET

Variable	Description/Range	Units
Surface type	Forest, shrub, savannas grassland and urban	—
LST	210.8–314.8	K
Brightness temperature	208.399–313.915	K
Solar zenith angle	25.69–178.95	Degree
Viewing angle	0–8	Degree

at 11 micron and 12 micron and associated with prescribed LST, geometry, surface type, and emissivities) are produced. A detailed introduction about the simulation datasets is given in Table III.

Noises at different levels are then added to the simulation datasets. The temperature uncertainties for different surface types are shown in Fig. 9. The LST uncertainty presents a similar upward trend for all land types as sensor noise increases. The uncertainty can be significant as high as 4 K if brightness temperature error reaches 1 K. Fig. 10 gives the results for emissivity retrievals. The emissivity uncertainty can reach as high as 0.13. Some surface types turn out to be more sensitive to sensor noise (e.g., shrubs and needle forest), while some land types stay at the same accuracy level even though the noise of BT is on the rise.

## VI. DISCUSSION

Some issues relevant to the new TES algorithm need further discussion. Singularity is a serious concern for the new algorithm. Equation (2) is theoretically solvable even when the two time measurements are slightly different. However, when the two measurements are too close in value, the solution would be inevitably significantly affected by the random noise in the data. Cautions, therefore, must be taken to avoid singularity of (2). First, the brightness temperatures ( $T_{11}$ ,  $T_{12}$ ) must be significantly different from different observation times to guarantee a reliable retrieval. Usually, a sufficient time interval between the observations can result in significant temperature difference. However, large time interval may break the emissivity constancy. Other authors experienced the similar problem. Watson (1992) pointed out that two-measurement method required distinct temperature and emissivity invariance, which is not easy to be satisfied at the same time, particularly for the polar-orbiting satellite data [35]. In our practice, the most stable results were obtained when the temporal interval between the two measurements is set in a range from one to three hours, which ensures sufficient temperature difference and emissivity constancy at the same time. Similar temporal interval is reported by Li *et al.* [13] and Yu *et al.* [9]. Second, the applied SW LST algorithms,  $F()$  and  $G()$ , should be independent. It is not sufficient to identify whether the two SW LST algorithms are independent from their formula. Experimental testing using actual satellite data is important as well. In this paper, we use two sets of the SW LST algorithms developed by Yu *et al.* [14], which is part of their LST algorithm development for the U.S. GOES-R satellite mission. The experimental results have demonstrated the feasibility of the MIA in practice.

It is worth mentioning that the time interval does not have to be fixed to a certain value (e.g., three hours) all the time. When the measurements at three-hour interval are not available for some reasons, such as cloudiness, the algorithm could automatically search for observations at other time stamps within the allowed time interval (one–three hours). Considering that geostationary satellites usually can provide high temporal observations (e.g., 15 min refresh rate of GOES Imager), more data pairs would be available for the MIA retrieval process. This flexible selection method will increase the number of qualified pairs of observations, which is of great value to operational production of LST product.

Further, even though multiple *in-situ* measurements (SURFRAD and ARM) were adopted for validation in this paper, the research on the mismatch of *in-situ* point measurement and satellite pixel observation was limited. Future studies will consider approaches that bridge the gap between point measurements and pixel observations. One possible way to deal with this scale disparity issue is building a spatial scaling model based on high resolution satellite data, such as ASTER or MODIS data.

Finally, we found that the solution for emissivity is not as stable as that for temperature, which may result in falsely retrieved emissivity, either negative or greater than one. The sensitivity to emissivity is understandable, which inherits

TABLE IV  
FORMULA AND COEFFICIENTS OF SPLIT-WINDOW ALGORITHMS

1) Formula		
No	Formula	Adaptation Reference
1	$T_s = C + (A_1 + A_2 \frac{1-\epsilon}{\epsilon} + A_3 \frac{\Delta\epsilon}{\epsilon^2})(T_{11} + T_{12})$ $+ (A_4 + A_5 \frac{1-\epsilon}{\epsilon} + A_6 \frac{\Delta\epsilon}{\epsilon^2})(T_{11} - T_{12}) + D(T_{11} - T_{12})(\sec\theta - 1)$	Wan & Dozier (1996)
2	$T_s = C + A_1 T_{11} + A_2(T_{11} - T_{12}) + A_3 \frac{1-\epsilon}{\epsilon} + A_4 \frac{\Delta\epsilon}{\epsilon^2} + D(T_{11} - T_{12})(\sec\theta - 1)$	Vidal (1991)
3	$T_s = C + A_1 T_{11} + A_2(T_{11} - T_{12}) + A_3(1 - \epsilon_{11}) + A_4 \Delta\epsilon$ $+ D(T_{11} - T_{12})(\sec\theta - 1)$	Coll & Valor (1997)
4	$T_s = C + A_1 T_{11} + A_2(T_{11} - T_{12}) + A_3(T_{11} - T_{12})\epsilon_{11}$ $+ A_4 T_{12} \Delta\epsilon + D(T_{11} - T_{12})(\sec\theta - 1)$	Price (1984)

\* Combination A is formed from Algorithm No. 1 and 2  
\* Combination B is formed from Algorithm No. 3 and 4

## 2) Coefficients

Daytime – Dry atmosphere								
No	C	A1	A2	A3	A4	A5	A6	D
1	1.535302	0.498186	0.059560	-0.146023	2.063007	1.340025	-1.889601	0.450768
2	0.659064	0.999553	1.593687	32.712996	-80.133336	-	-	0.451102
3	0.625987	0.999581	1.593094	34.802239	-66.959970	-	-	0.451273
4	1.382718	0.999334	7.431078	-5.998309	-0.352476	-	-	0.469732
Daytime – Moist atmosphere								
No	C	A1	A2	A3	A4	A5	A6	D
1	-4.154069	0.506508	0.052156	-0.116443	2.605759	-0.159998	4.670031	0.377953
2	-4.963992	1.015891	2.082987	29.976879	-60.828114	-	-	0.378838
3	-4.989946	1.015908	2.082698	31.806553	-48.164224	-	-	0.378961
4	-4.443319	1.016381	17.367623	-15.632429	-0.208873	-	-	0.387167
Nighttime – Dry atmosphere								
No	C	A1	A2	A3	A4	A5	A6	D
1	0.188587	0.500759	0.059167	-0.162152	1.954092	1.314697	7.809722	0.463188
2	-0.655825	1.004673	1.460630	32.057728	-85.508048	-	-	0.464989
3	-0.683713	1.004681	1.459900	34.157634	-72.925987	-	-	0.465384
4	0.215850	1.003838	7.180705	-5.865579	-0.381284	-	-	0.473137
Daytime – Moist atmosphere								
No	C	A1	A2	A3	A4	A5	A6	D
1	12.904747	0.476807	0.051345	-0.112504	3.025176	-0.951041	2.529027	0.421439
2	12.192170	0.956169	2.522419	28.736995	-62.534230	-	-	0.421464
3	12.168215	0.956179	2.522171	30.515867	-50.602618	-	-	0.421552
4	12.555472	0.957078	16.607601	-14.416924	-0.237603	-	-	0.432226

\*Daytime: Solar zenith < 85 degree; Night time: Solar zenith >= 85 degree  
\*Dry atmospheric condition: atmospheric total column water vapor <=2.0 g/cm<sup>2</sup>  
Moist atmospheric condition: atmospheric total column water vapor > 2.0 g/cm<sup>2</sup>

from the problem that most SW LST algorithms suffer. Yu *et al.* [14] analyzed the emissivity sensitivities of nine SW LST algorithms and indicated that small uncertainty in emissivity could cause significant uncertainty in LST retrievals (over 3 K). One option to minimize the effect brought by uncertainty in emissivity is to find the optimal combination from those SW LST algorithms that are less sensitive to emissivity. According to the previous research, SW algorithms developed by Prata *et al.* and Ulivieri *et al.* [14] showed low sensitivity to emissivity since the emissivity difference is not introduced in the algorithms.

## VII. CONCLUSION

According to the unique characteristics of geostationary satellite observations (e.g., GOES, SEVIRI) with frequent observations, the MIA was presented in detail to retrieve temperature and emissivity simultaneously from two-time TIR observations of geostationary satellites. Examples were given to show how to derive LST and LSE from the MSG/SEVIRI

and GOES/Imager data. The new method has the advantage of simplicity in using two measurements within a period of time without having to solve radiative transfer equations. The flexibility of integration of the established LST retrieval algorithms makes the method easy to implement. Two combinations of SW LST algorithms were adapted in this method, and both produce satisfactory retrieval results. Validation results demonstrated that the TES algorithm is capable of simultaneously deriving qualified LST and LSE with good retrieval precision.

Further study is necessary for the completeness and practicality of this algorithm. First, only two combinations of SW LST algorithms have been selected and implemented here. Combinations of other existing SW LST algorithms are also feasible in theory and effective in practice, but their retrieval precision and stability need to be examined.

Second, singularity is still the major concern for the new algorithm. More experience in future is needed to gain deeper understanding on how to choose optimal data pairs with both independent temperatures and constant emissivity. Finally, this algorithm is assumed to be applicable to the next generation

of GOES-R satellites. Even though it works well in the test of GOES-8 data, other problems may occur when applied to the actual GOES-R data. The MIA would probably need to be adjusted to the specific characteristics of GOES-R data in practice.

#### APPENDIX

Formula and coefficients of split-window algorithms are shown in Table IV.

#### REFERENCES

- [1] S. W. Running, C. O. Justice, V. Salomonson, D. Hall, J. Barker, Y. J. Kaufmann, A. H. Strahler, A. R. Huete, J.-P. Muller, V. Vanderbilt, Z. M. Wan, P. Teillet, and D. Carneggie, "Terrestrial remote sensing science and algorithms planned for EOS/MODIS," *Int. J. Remote Sens.*, vol. 15, no. 17, pp. 3587–3620, 1994.
- [2] Z. L. Li, F. Becker, M. P. Stoll, and Z. Wan, "Evaluation of six methods for extracting relative emissivity spectral from thermal infrared images," *Remote Sens. Environ.*, vol. 69, pp. 197–214, Sep. 1999.
- [3] Z. L. Li and F. Becker, "Feasibility of land surface temperature and emissivity determination from AVHRR data," *Remote Sens. Environ.*, vol. 43, no. 1, pp. 67–85, Jan. 1993.
- [4] S. Liang, "An optimized algorithm for separating land surface temperature and emissivity from multispectral thermal infrared imagery," *IEEE Trans. Geosci. Remote Sens.*, vol. 39, no. 2, pp. 264–274, Feb. 2001.
- [5] K. Watson, "Spectral ratio method for measuring emissivity," *Remote Sens. Environ.*, vol. 42, no. 2, pp. 113–116, Nov. 1992.
- [6] P. S. Kealy and A. R. Gabell, "Estimation of emissivity and temperature using Alpha Coefficients," in *Proc. 2nd TIMS Workshop*, 1990, pp. 234–239.
- [7] Z. Wan and Z. L. Li, "A physics-based algorithm for retrieving land-surface emissivity and temperature from EOS/MODIS data," *IEEE Trans. Geosci. Remote Sens.*, vol. 35, no. 4, pp. 980–996, Jul. 1997.
- [8] A. R. Gillespie, S. Rokugawa, T. Matsunaga, J. S. Cothren, S. Hook, and A. B. Kahle, "Temperature and emissivity separation from advanced spaceborne thermal emission and reflection radiometer (ASTER) images," *IEEE Trans. Geosci. Remote Sens.*, vol. 36, no. 4, pp. 1113–1126, Jul. 1998.
- [9] Y. Yu, H. Xu, D. Tarpley, and M. Goldberg, "A simplified method for measuring land surface temperature and emissivity using thermal infrared split-window channels," in *Proc. IGARSS Annu. Meeting*, Jul. 2009, p. 1830.
- [10] K. Mao, J. Shi, H. Tang, Z.-L. Li, X. Wang, and K.-S. Chen, "A neural network technique for separating land surface emissivity and temperature from ASTER imagery," *IEEE Trans. Geosci. Remote Sens.*, vol. 46, no. 1, pp. 200–208, Jan. 2008.
- [11] L. F. Peres and C. C. DaCamara, "Improving two-temperature method retrievals based on a nonlinear optimization approach," *IEEE Trans. Geosci. Remote Sens.*, vol. 3, no. 2, pp. 232–236, Apr. 2006.
- [12] L. F. Peres and C. C. DaCamara, "Land surface temperature and emissivity estimation based on the two-temperature method: Sensitivity analysis using simulated MSG/SEVIRI data," *Remote Sens. Environ.*, vol. 91, pp. 377–389, Jun. 2004.
- [13] J. Li and T. Schmit, *GOES-R Advanced Baseline Imager (ABI) Algorithm Theoretical Basis Document for Surface Emissivity*. Madison, WI, USA: CIMSS, 2008.
- [14] Y. Yu, D. Tarpley, J. L. Privette, M. D. Goldberg, M. K. Rama Varma Raja, K. Y. Vinnikov, and H. Xu, "Developing algorithm for operational GOES-R land surface temperature product," *IEEE Trans. Geosci. Remote Sens.*, vol. 47, no. 3, pp. 936–951, Mar. 2009.
- [15] Z. Wan and J. Dozier, "A generalized split-window algorithm for retrieving land-surface temperature from space," *IEEE Trans. Geosci. Remote Sens.*, vol. 34, no. 4, pp. 892–905, Jul. 1996.
- [16] Y. Yu, J. L. Privette, and A. C. Pinheiro, "Evaluation of split-window land surface temperature algorithms for generating climate data records," *IEEE Trans. Geosci. Remote Sens.*, vol. 46, no. 1, pp. 179–192, Jan. 2008.
- [17] A. Vidal, "Atmospheric and emissivity correction of land surface temperature measured from satellite using ground measurements or satellite data," *Int. J. Remote Sens.*, vol. 12, no. 12, pp. 2449–2460, 1991.
- [18] C. Coll and V. Caselles, "A split-window algorithm for land surfaces temperature from advanced very high-resolution radiometer data: Validation and algorithm comparison," *J. Geophys. Res.*, vol. 102, no. D14, pp. 16697–16713, Jan. 1997.
- [19] F. Barker and Z. L. Li, "Toward a local split window method over land surface," *Int. J. Remote Sens.*, vol. 3, no. 3, pp. 369–393, 1990.
- [20] V. Caselles, C. Coll, and E. Valor, "Land surface temperature determination in the whole Hapex-Sahell area from AVHRR data," *Int. J. Remote Sens.*, vol. 18, no. 5, pp. 1009–1027, 1997.
- [21] C. Coll, V. Caselles, J. A. Sobrino, and E. Valor, "On the atmospheric dependence of the split-window equation for land surface temperature," *Int. J. Remote Sens.*, vol. 15, no. 1, pp. 1915–1932, 1994.
- [22] A. J. Prata, "Land surface temperatures derived from the advanced very high resolution radiometer and the along-track scanning radiometer. 2: Experimental results and validation of AVHRR algorithms," *J. Geophys. Res.*, vol. 99, no. D6, pp. 13025–13058, Jan. 1994.
- [23] J. C. Price, "Land surface temperature measurements from the split window channels of the NOAA-7 AVHRR," *J. Geophys. Res.*, vol. 79, pp. 5039–5044, Feb. 1984.
- [24] J. A. Sobrino, Z.-L. Li, M. P. Stoll, and F. Becker, "Improvements in the split-window technique for land surface temperature determination," *IEEE Trans. Geosci. Remote Sens.*, vol. 32, no. 2, pp. 243–253, Mar. 1994.
- [25] C. Ulivieri and G. Cannizzaro, "Land surface temperature retrievals from satellite measurements," *Acta Astron.*, vol. 12, no. 12, pp. 985–997, Dec. 1985.
- [26] C. Ulivieri, M. M. Castronuovo, R. Francioni, and A. Cardillo, "A SW algorithm for estimating land surface temperature from satellites," *Adv. Space Res.*, vol. 14, no. 3, pp. 59–65, Mar. 1992.
- [27] Z. Wan, "New refinements and validation of the MODIS land-surface temperature/emissivity products," *Remote Sens. Environ.*, vol. 112, no. 1, pp. 59–74, Jan. 2008.
- [28] D. A. Faysash and E. A. Smith, "Simultaneous land surface temperature-emissivity retrieved in the infrared split window," *J. Atmospheric Ocean. Technol.*, vol. 16, no. 11, pp. 1673–1689, Nov. 1999.
- [29] D. Sun and R. Pinker, "Estimation of land surface temperature from a geostationary operational environmental satellite (GOES-8)," *J. Geophys. Res.*, vol. 108, no. D11, p. 4326, Jun. 2003.
- [30] R. Pinker, T. Sun, D. Hung, M.-P. Li, C. Basara, and B. Jeffrey, "Evaluation of satellite estimates of land surface temperature from GOES over the United States," *J. Appl. Meteorol. Climatol.*, vol. 48, no. 1, pp. 167–180, Jan. 2009.
- [31] D. Flynn and G. Hodges, "Multi-filter radiometer (MFR) handbook," U.S. Dept. Energy, Office Sci., Office Biol. Environ. Res., Washington, DC, USA, Tech. Rep. DOE/SC-ARM/TR-059, Feb. 2005.
- [32] R. A. Pepller, P. J. Lamb, and D. L. Sisterson, "Site scientific mission plan for the Southern Great Plains CART site: January–June 1996," Nat. Tech. Inf. Services Rep. ARM-96-002, IL, USA, p. 86, Jun. 1996.
- [33] J. A. Augustine, J. J. DeLuisi, and C. N. Long, "SURFRAD—A national surface radiation budget network for atmospheric research," *Bull. Amer. Meteorol. Soc.*, vol. 81, no. 10, pp. 2341–2357, 2000.
- [34] J. A. Augustine, G. B. Hodges, C. R. Cornwall, J. J. Michalsky, and C. I. Medina, "An update on SURFRAD—The GCOS surface radiation budget network for the continental United States," *J. Atmos. Ocean. Technol.*, vol. 22, no. 10, pp. 1460–1472, 2005.
- [35] K. Watson, "Two-temperature method for measuring emissivity," *Remote Sens. Environ.*, vol. 42, no. 2, pp. 117–121, 1992b.



**Li Fang** received the B.Sc degree in geographic information systems from Wuhan University, Hubei, China, in 2005, the M.Sc. in geographic and cartographic sciences and the Ph.D. degree in earth system and geoinformation sciences from George Mason University (GMU), Fairfax, VA, USA, in 2011 and 2012, respectively.

She was a Research Assistant with the Chinese Academy of Sciences, Beijing, China, for three years, and became a Ph.D. candidate in cartography and geographical information system. She is currently a Research Associate with the National Environmental Satellite, Data, and Information Service Center for Satellite Applications and Research, National Oceanic and Atmospheric Administration, College Park, MD, USA. Her current research interests include reversion and applications of land surface temperature (LST). She engaged in NOAA PSID projects as a key member to develop a software package for operational Geostationary Operational Environmental Satellite LST product.



**Yunyue Yu** received the B.Sc. degree in physics from the Ocean University of Qingdao (OUQ), Qingdao, China, in 1982, the M.Sc. degree equivalent in advanced physics from Peking University, Beijing, China, in 1986, and the Ph.D. degree in aerospace engineering sciences from the University of Colorado (CU), Boulder, CO, USA, in 1996.

He was a Lecturer and an Associate Professor, during his tenure with OUQ from 1982 to 1993, and held leadership roles in multiple international corporation projects. From 1987 to 1992, he was a

Visiting Scientist with the University of Dundee, Dundee, U.K., the Division of Atmospheric Research, Australian Commonwealth Scientific and Industrial Research Organization, and the Colorado Center for Astrodynamics Research, CU. In 1996, he was with the Earth Observation System Satellites Program through Raytheon ITSS and George Mason University and with NASA Goddard Space Flight Center. Currently, he is a Physical Scientist with the National Environmental Satellite, Data, and Information Service Center for Satellite Applications and Research, National Oceanic and Atmospheric Administration, College Park, MD, USA, the Chairman of the land surface algorithms working group of the GOES-R satellite mission, and a member of the National Polar-orbiting Operational Environmental Satellite System Visible/Infrared Imager Radiometer Suite Operational Algorithm Team. He has accomplished a variety of projects in ocean and land surface remote sensing and applications.



**Donglian Sun** received the Ph.D. degree from the University of Maryland, College Park, MD, USA, in 2003.

She is currently a Faculty Member with the Department of Geography and Geoinformation Science, George Mason University, Fairfax, VA, USA. Her current research interests include information retrieval from remotely sensed data, numerical model simulations of tropical storms, and remote-sensing applications to coastal problems.



**Hui Xu** received the B.Sc. degree in geography from Beijing University, Beijing, China, the M.Sc. degree in land and water management from the Cranfield Institute of Technology, Cranfield, U.K., and the Ph.D. degree in geography from the University of Edinburgh, Edinburgh, U.K.

She has worked in remote sensing data application, research and product development, as well as integration of remote sensing and GIS. She was a Project Scientist for snow mapping and snow depth monitoring with the University of Bristol, Bristol,

U.K. Her work at Nottingham University, Nottingham, U.K., on monitoring leaf area of sugar beet using ERS-1 SAR data contributed to a yield prediction project for the British Sugar. She taught remote sensing and GIS courses as an Assistant Professor with Frostburg State University, Frostburg, MD, USA, before joining IMSS, Inc., MD, in 2001. Since then, she has been with the NOAA/NESDIS/STAR on various projects, including re-hosting, documentation and validation of the automatic snow mapping system, on-orbit verification and inter-satellite calibration of NOAA polar-orbiting radiometers, and her participation in the GOES-R algorithm development and testing of NDVI and LST products in the Land Application Team.